Available online at www.sciencedirect.com
ScienceDirect
Journal of the European Ceramic Society 27 (2007) 4697–4703
www.elsevier.com/locate/jeurceramsoc

Suppression of elastically accommodated grain-boundary sliding in high-purity MgO

Auke Barnhoorn *, Ian Jackson, John D. Fitz Gerald, Yoshitaka Aizawa

Research School of Earth Sciences, Australian National University, ACT 0200, Australia

Received 18 October 2006; received in revised form 22 March 2007; accepted 6 April 2007
Available online 11 June 2007

Abstract

The first high-temperature mechanical spectroscopy experiments on high-purity polycrystalline MgO reveal a monotonically frequency- and temperature-dependent dissipation 'background'—without any evidence of the superimposed dissipation peak observed in a previous study of a specimen of lower-purity [Webb, S. and Jackson, I. *Phys. Chem. Min.*, 2003 **30**, 157]. The dissipation and associated relaxation of the shear modulus observed in both studies are well described in an internally consistent manner by a novel Burgers-type model based on a creep function incorporating suitable distributions of anelastic relaxation times. The contrasting patterns for the two materials reinforce an emerging generalisation concerning high-temperature viscoelastic behaviour, whereby the presence of a secondary intergranular phase of relatively low viscosity, and the associated rounding of grain edges, is apparently required to allow elastically accommodated grain-boundary sliding. The absence, in sufficiently pure polycrystalline materials, of a dissipation peak attributable to elastically accommodated grain-boundary sliding is in conflict with classical micromechanical models for grain-boundary sliding, which are therefore being revisited.

Keywords: Mechanical properties; MgO; Grain boundaries; Structural applications; Viscoelasticity

1. Introduction

The high-temperature breakdown of strictly elastic behaviour in fine-grained materials is usually attributed to grain-boundary sliding facilitated by the low effective viscosity of the thin grain-boundary region. Such sliding on a non-planar grain-boundary produces incompatibilities that must be accommodated under conditions of low stress either by elastic distortion of the sliding grains or by diffusion. In the classic Raj–Ashby theory of grain-boundary sliding,[2,3] it is envisaged that sliding with elastic accommodation occurs at moderate temperatures and that the onset of diffusion at higher temperatures allows transient and ultimately steady-state diffusional creep. As a first indication of departure from elastic behaviour, sub-resonant forced-oscillation tests performed at progressively higher temperatures should therefore reveal the pronounced dissipation peak (and associated shear modulus relaxation) predicted for elastically accommodated sliding.[2] This should be followed at higher temperatures by the monotonically temperature and frequency-dependent background associated with transient and steady-state diffusional creep. Observations of dissipation peaks either precursory to, or superimposed upon high-temperature background have commonly been attributed to elastically accommodated sliding.[4–7] During the past decade, however, there have also been intriguing reports of high-temperature viscoelastic behaviour consisting of background only without any well-resolved dissipation peak—in disagreement with the classical theory.[2] Background-only behaviour in Si_3N_4 and hexagonal BN, SiC[8–10] and olivine[11] is observed only in the absence of a widely dispersed low viscosity grain-boundary phase. Similarly, for alumina lacking a glassy grain-boundary phase, the dissipation Q^{-1} varies monotonically with oscillation period T_o and temperature T.[12,13] The variation of Q^{-1} with the pseudo-frequency master variable $X = T_o \exp(-E/RT)$ becomes progressively milder with decreasing X without a peak that is clearly distinguishable from the background.

As part of a broader campaign to reconcile the micromechanical description of grain-boundary sliding with experimental observations, we are undertaking a comprehensive study of the high-temperature viscoelastic behaviour of polycrystalline

* Corresponding author. Tel.: +61 2 6125 2494.
E-mail address: auke.barnhoorn@anu.edu.au (A. Barnhoorn).

0955-2219/$ – see front matter © 2007 Elsevier Ltd. All rights reserved.
doi:10.1016/j.jeurceramsoc.2007.04.005

MgO. Our ultimate goal is to provide tight constraints not only on the frequency–temperature dependence of both modulus and dissipation but also to document their grain size sensitivities and the relationship with key grain-boundary nanostructures. Here we report results of the first torsional forced-oscillation measurements on a dense polycrystalline specimen of high-purity MgO. Comparison with previous results for an impure MgO specimen[1] provides a test of the generality of the association between a pronounced high-temperature dissipation peak and the presence of a grain-boundary phase of low viscosity.

2. Experimental

For fabrication of the samples, high-purity (>99.99 wt.%) MgO nanopowder with a grain size of 45–60 nm (supplied by Ube Materials Industries Ltd.) has been used. A sample with low porosity ($\phi < 1\%$) and 5–10 μm grain size has been obtained by a four-stage fabrication process: (1) cold-isostatic pressing at 200 MPa for 0.5 h to yield samples of ∼50% porosity, (2) pressureless sintering at 1100 °C for 2 h in an N_2-rich environment to evaporate residual CO_2 and H_2O followed by slow cooling at 2 °C/min to prevent sample cracking ($\phi \sim 40\%$), (3) hot-isostatic pressing of the sample in a steel jacket in a gas-medium apparatus at 300 MPa argon confining pressure and 1100 °C for 24 h for further densification of the sample ($\phi \sim 1\%$.), immediately followed by (4) second stage hot-isostatic pressing again at 300 MPa, but now at 1300 °C for 24 h to enhance grain growth (to 5 μm) and further reduction in porosity (Table 1).

Variations of conditions for hot-isostatic pressing revealed that porosity reduction was most efficient at the relatively low temperature of 1100 °C due to the absence of significant grain growth ($T/T_m \sim 0.35$, $T_m = 2900$ °C[14]), similar to previous observations.[15] At 1300 °C, more rapid grain growth results in preservation of pore space, which impedes efficient reduction of porosity. Average H_2O contents for the bulk specimen (both structurally bound water and water adsorbed on the grain boundaries) of the hot-isostatically pressed and mechanically tested samples (sections 285 μm thick) were determined by Fourier transform infrared spectroscopy (FTIR).[16] MgO sample densities were measured with the Archimedean method and compared with the theoretical density of MgO ($\rho = 3.584$ g/cm^3), resulting in an estimate of the inaccessible porosities. Grain sizes and crystallographic preferred orientations (CPO) were determined by electron backscatter diffraction (EBSD) mapping with a step size of 0.6 μm for the hot-isostatically pressed specimen (#6562) and 0.75 μm for the same specimen recovered after mechanical testing (#1077) and grain boundaries identified by a misorientation angle greater than 10°. Average grain sizes correspond to the mean of the log-normal distributions of equivalent diameters.

Table 1
Experimental and microstructural characteristics of samples 6562 and 1077

	Hot-isostatic pressing	Forced-oscillation
Experiment	6562	1077
Pressure (MPa)	300	200
Temperature (°C)	1100/1300	20–1300
Duration (h)	24/24	–
Oscillation period (s)	–	1–1000
H_2O content (ppm)	50	<1
Porosity (%)	0.96 ± 0.01	0.55 ± 0.04
Grain size (μm)	5.2	8.8

The hot-isostatically pressed sample was precision ground to cylindrical shape (length = 30.00 ± 0.02 mm, diameter = 11.50 ± 0.02 mm). This sample was fired prior to mechanical testing at 1100 °C for 2 h in a N_2-rich environment to vapourise any H_2O remaining after grinding. Torsional forced-oscillation experiments were conducted at 200 MPa confining pressure over the temperature range of 20–1300 °C (Table 1).[17] Sinusoidally varying stresses were applied at 10 different periods between 1 and 1000 s at torque amplitudes equivalent to maximum shear stresses of 0.3 MPa, resulting in maximum shear strains of 3×10^{-5} at the highest temperature. The mechanical data have been corrected for contributions of the mechanical assembly (pistons, metal foils and steel jacket) to the mechanical behaviour. Before performing routine torsional forced-oscillation measurements the sample was annealed in situ at 200 MPa confining pressure and 1300 °C for 47 h. The mechanical behaviour was monitored during annealing. Small changes in shear modulus G and strain-energy dissipation Q^{-1} with annealing time reflect minor microstructural changes (grain size increased from 5 to 9 μm, and porosity decreased from 1 to 0.55%). Such microstructural evolution is plausibly confined to the highest temperature, so that mechanical data subsequently acquired during staged cooling pertain to a constant microstructure. The raw forced-oscillation data were converted into shear modulus G, strain-energy dissipation Q^{-1} and shear strain[18] for each period at all temperatures. Combined G and Q^{-1} data for temperatures of 900–1300 °C were least-squares fitted to an extended Burgers model[19,20] (Table 2). This global modeling allows for the possible presence of a dissipation peak as well as a frequency-dependent dissipation background by incorporating alternative distributions of anelastic relaxation times.

3. Results

The mechanically tested sample shows lines of pores inside large grains, which are remnants of old grain boundaries indicating slight grain growth during the course of the experiment (Fig. 1c and d). Backscattered electron images also show that porosity is restricted to grain-boundary triple junctions and interiors of grains. The sample has an equilibrated microstructure of grain boundaries (Fig. 1a and c). FTIR measurements indicate that the small amount of H_2O (∼50 ppm) in the hot-isostatically pressed sample (#6562) has disappeared completely during the course of the 1300 °C annealing prior to the forced-oscillation experiment (H_2O contents below detection limit, <1 ppm). EBSD analyses show that the MgO grains have a random distribution of crystallographic orientations (Fig. 1f). The sample is an isotropic material due to its random CPO and the absence of any preferred grain-boundary alignment.

As expected from the pure MgO starting powder (>99.99% MgO), no secondary phases could be found either in scanning

Table 2
Optimal values of the parameters for the extended Burgers model least-squares fitted (without and with a dissipation peak) to the data for the high-purity specimen of this study and the specimen of lower-purity,[1] respectively

	High-purity MgO (this study) *background only* 900–1300 °C (±)		Lower-purity MgO[1] *background + peak* 800–1300 °C (±)	
T_{ref} (°C)	900		800	
J_u (GPa^{-1})	9.98E−03	7.40E−05	1.12E−02	1.25E−04
$(\delta \ln J_u/\delta T)_r$ (°C^{-1})	1.17E−03	6.59E−05	2.07E−05	1.50E−04
Δ_b	2.00E+00		2.00E+00	
α	2.57E−01	8.07E−03	2.73E−01	1.31E−02
log τ_{LR}	6.70E−01	3.88E−02	−2.00E+00	
log τ_{HR}	5.38E+00	5.81E−02	5.07E+00	1.37E−01
log τ_{MR}	5.01E+00	6.25E−02	4.77E+00	1.46E−01
Δ_{po}	–		9.69E−01	6.36E−02
log τ_{PR}	–		6.65E+00	4.45E−01
σ	–		3.83E+00	3.90E−01
E_B (J mol^{-1})	3.25E + 05	5.70E+03	2.26E+05	1.02E+04
E_P (J mol^{-1})	–		8.05E+05	5.35E+04
Number of measurements	178		140	
χ^2 (G)	150.40		141.89	
χ^2 (Q^{-1})	173.95		30.50	
χ^2 (total)	324.35		172.39	

The model for the frequency dependence of G and Q^{-1} is the Laplace transform of a Burgers-type creep function constructed as the sum of three terms: (i) an unrelaxed compliance J_U with a temperature dependence prescribed by the value of $\delta \ln J_U/\delta T$; (ii) an anelastic contribution based on a distribution $D_B(\tau) \sim \tau^{\alpha-1}$ [for $\tau_L(T) < \tau < \tau_H(T)$] to describe the high-temperature background and a superimposed Gaussian distribution of relaxation times $D_P(\tau) \sim \exp\{-[\ln(\tau/\tau_P(T))/\sigma]^2/2\}$ if required for any dissipation peak and (iii) steady-state Newtonian creep with specified viscosity η or Maxwell time $\tau_M(T) = \eta J_U$. Each of the relaxation times τ_L, τ_H, τ_M and τ_P has an Arrhenian temperature dependence with an appropriate activation energy (E_B for τ_L, τ_H, andτ_M) and E_P for τ_P (for further details of the model, see Ref. 20).

electron microscopy observations or at very high magnification in the transmission electron microscope (TEM). No grain boundaries or triple junctions show any microstructure suggesting impurities (Fig. 2a). Grain-boundary images are thin, 3–4 nm in width and often gently curved. TEM does show that ∼70% of the triple junctions have pores with sizes of 100 nm to 2 μm. The remaining ∼30% of the triple junctions are closed. While we have no information about fluid in the pore spaces throughout the mechanical tests, these microstructures are likely to be at least partially connected, consistent with the loss of H_2O detected by FTIR. Very few dislocations are present in the MgO grains (Fig. 2b) with a dislocation density of $\rho \sim 10^{-12}$ m^{-2}. Patches of submicron grains still occur between the μm-sized MgO grains. Those very small grains have a larger dislocation density, probably introduced during the earlier cold-isostatic pressing stage of the sample preparation procedure. Dislocations

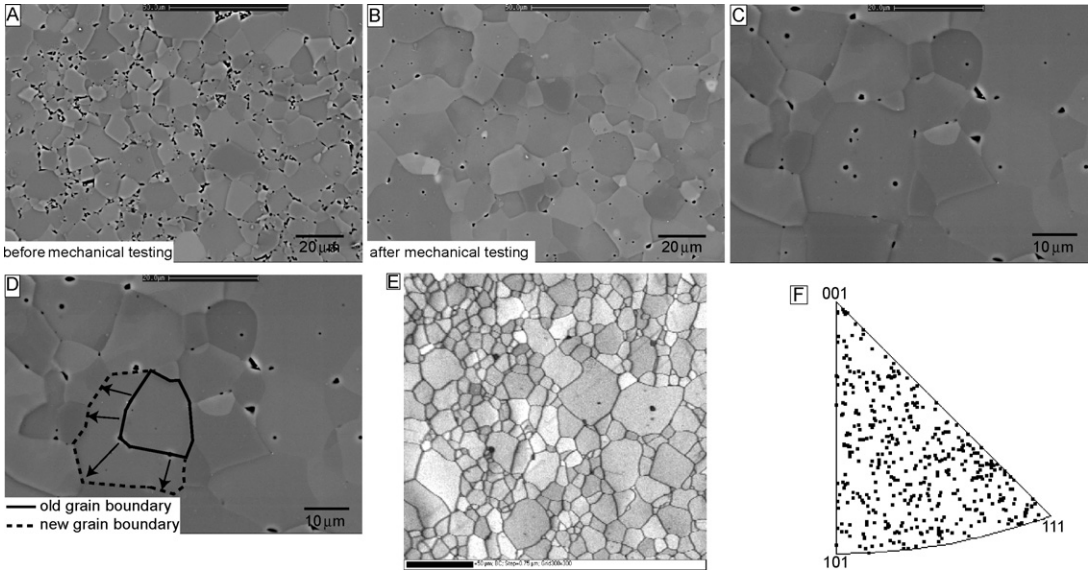

Fig. 1. SEM backscattered electron images of (A) MgO sample (6562) after hot-isostatic pressing, (B) after 3 weeks of high-temperature mechanical testing (1077), (C and D) detail of sample 1077 highlighting grain growth and aligned intergranular porosity, (E) EBSD pattern contrast map of sample 1077. Grain boundaries have low pattern contrast. (F) Inverse pole figure along the x-direction showing the random distribution of orientations.

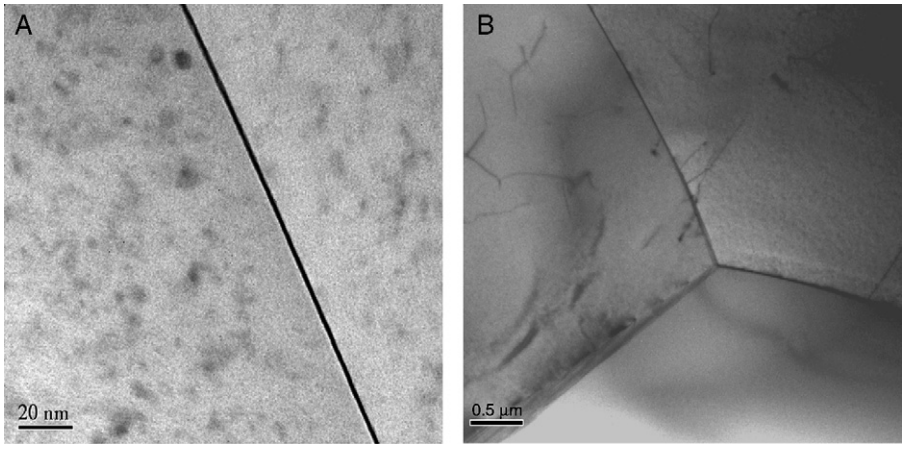

Fig. 2. TEM images of sample 1077. (A) High magnification image of a typical grain-boundary, carefully tilted parallel to the electron beam to show an image width of ∼2 nm and a lack of secondary phases along the boundary and (B) image of a grain-boundary triple junction, where no pore space is present. Some dislocations are present in the grain interiors.

in those high density areas are often tangled and form dislocation walls.

MgO behaves essentially elastically over the accessible range of oscillation periods (1–1000 s) at temperatures ≤800 °C, as is evident from the frequency-independent G and minimal Q^{-1} (Fig. 3). The resulting G of 125 GPa at 20 °C is slightly less than 132 GPa calculated for an ideal polycrystal from single-crystal elastic constants.[21] This difference in G presumably reflects the presence of the small volume fraction of residual pores in the polycrystalline material. Variations in confining pressure have no effect on the elastic behaviour of the specimen, indicating the virtual absence of crack porosity. At temperatures above 800 °C, pronounced departures from elastic behaviour are evident in the intense dissipation Q^{-1} and associated frequency dependence (dispersion) of the shear modulus G (Fig. 3a and b). Anelastic and viscous contributions to the deformation, distinguished through complementary torsional microcreep tests, increase with increasing oscillation period and temperature. Maximum reduction in G between 1 and 1000 s occurs at 1300 °C and is 70%. The systematic monotonic variations in G and Q^{-1} exclude the presence of any localised dissipation peak of significant height on top of the frequency-dependent dissipation background. An extended Burgers model that incorporates a suitably broad distribution of anelastic relaxation times instead of a localised dissipation peak provides an internally consistent fit to all of the G and Q^{-1} data for temperatures of 900–1300 °C ($\chi^2 = 324$ for $N = 178$, Fig. 3a and b and Table 2). We are not aware of previous reports of the fitting of both G and Q^{-1} of mechanical spectroscopy data to such a creep-function-based viscoelastic model for ceramic materials.

4. Discussion

Mechanical data for the high-purity polycrystalline MgO of the present study contrasts markedly with those for MgO polycrystals of lower-purity[1] (Fig. 3c and d). High-purity MgO has monotonically frequency-dependent Q^{-1} values with no evidence of a superimposed dissipation peak (Fig. 3a–c and Table 2). On the contrary, the Q^{-1} data previously measured for MgO[1] show a clear dissipation peak superimposed on the frequency-dependent dissipation background in the 900–1300 °C temperature range (Fig. 3d). We have newly fitted these Webb and Jackson's[1] G and Q^{-1} data[1] to extended Burgers models, with and without a localised peak modeled with an extra Gaussian distribution of anelastic relaxation times (Table 2). Incorporation of a localised dissipation peak resulted in a much better fit ($\chi^2 = 172$) than with a broad dissipation background only ($\chi^2 = 857$). The dissipation peak evident in the results for the impure MgO material,[1] but absent from those for this new specimen of much higher purity, is associated with the presence of a fluid containing dissolved silica and other impurities such as Ca and Mg[1] dispersed along grain boundaries. Post-mortem investigations of the sample in a scanning electron microscope[1] revealed crystals of the secondary phase forsterite, and smaller Mg–Ca phases and fibrous secondary phases, presumably precipitated from the intergranular fluid during staged cooling. Infrared-spectra analyses indicated that the latter two phases are most likely carbonate and brucite.

The association between high-temperature grain-boundary dissipation peaks and the presence of low viscosity grain-boundary phases has been most thoroughly documented by Pezzotti and his colleagues. As the result of inadvertent oxidation, polycrystalline specimens of silicon nitride and silicon carbide typically contain a small amount of SiO_2 impurity—generally present as a nm-thick glassy film wetting grain boundaries. The high-temperature dissipation peak observed in torsional pendulum experiments on each of these materials[8,10] and hexagonal BN containing a $CaO–B_2O_3$ glassy phase,[9] was attributed to elastically accommodated grain-boundary sliding. However, the height of the dissipation peak is consistently much less than predicted by the Raj–Ashby theory,[2,5] requiring the inclusion of an adjustable 'boundary-shape' parameter much smaller than the value given by Raj and Ashby.[2] Corresponding materials that lack the amorphous grain-boundary phase display no high-temperature dissipation peak—only a reduced level of exponentially temperature-

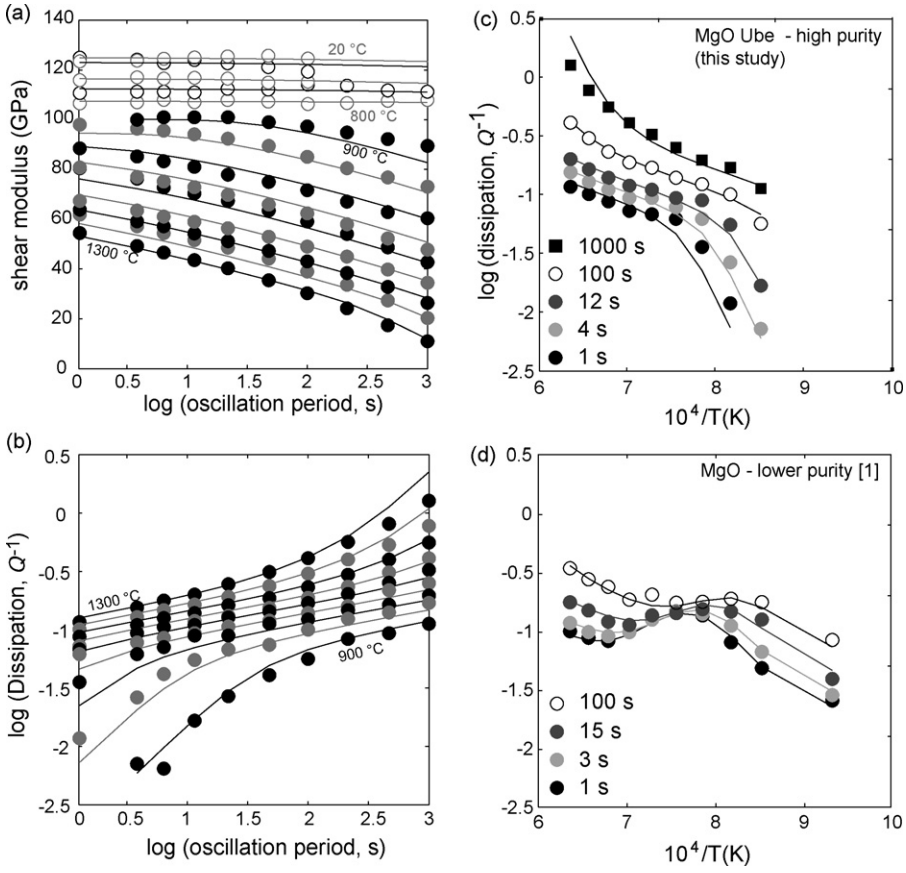

Fig. 3. Variation with oscillation period of (A) G between 20 and 1300 °C and (B) Q^{-1} between 900 and 1300 °C. Solid lines represent the least-squares fit of the extended Burgers model [15,16] between 900 and 1300 °C using a dissipation background only. Alternating grey and black symbols indicate temperature steps of 50 °C. G and Q^{-1}data between 20 and 800 °C (open symbols) have not been included in the extended Burgers model. Best-fit values of Burgers model parameters are stated in Table 2. (C and D) Variation with $1/T$ of Q^{-1} for high-purity MgO (this study) and lower-purity MgO[1], respectively.

dependent background.[8,10] The authors suggested that the absence of a dissipation peak implies that (elastically accommodated) grain-boundary sliding is inhibited either by the higher viscosity of the boundary region or by tighter interlocking of grains at grain-edge triple junctions.

The presence of a pronounced dissipation peak for ferromagnesian silicate olivine has similarly been linked to a grain-boundary phase of low viscosity.[7,11] with a systematic positive correlation between peak height and alumino-silicate melt fraction. Importantly, the alumino-silicate melt does not wet olivine grain boundaries. While elastically accommodated sliding is inhibited in the melt-free olivine by grain interlocking, it is argued to be facilitated in the melt-bearing material not by lowered grain-boundary viscosity but by rounding of grain edges at triple junction tubules.[7] This suggestion is supported by the marked decrease of the modeled relaxation strength Δ estimated for elastically accommodated grain-boundary sliding from ~0.8 for close-packed spheres[4,22] compared to ~0.23 for space-filling hexagonal grains.[23] Similarly, the relaxation strength estimated by Raj and Ashby[2] decreases logarithmically towards zero with increasing N, the number of terms retained in the Fourier series representation of the boundary topography.[24] It follows that the interlocking of sharp grain edges in sufficiently pure materials, described by $N \rightarrow \infty$, might inhibit elastically accommodated grain-boundary sliding.

In the absence of a glassy grain-boundary phase, fine-grained polycrystalline alumina[12] displays dissipation Q^{-1} that is smoothly monotonic over almost eight decades variation of the pseudo-period master variable $X = T_o \exp(-E/RT)$, see also.[11,25] This approach which involves the consistent translation along the period axis of the entire isothermal spectrum with changing temperature is equally applicable to the MgO data of the present study (Fig. 4). The sigmodial Q^{-1} (X) curve for MgO accommodates the full extent of a broad anelastic absorption band at moderate values of X from the lower edge of the absorption band ($X \sim 10^{-13}$ s) to the onset of appreciably viscous deformation tending to a slope of 1 for $X > 10^{-9}$ s in the master variable spectrum. This behaviour indicates that viscoelasticity needs to be modeled as an intimate mixture of recoverable (anelastic) and permanent (viscous) strains with a Burgers-type model, thereby reinforcing the conclusion of Lakki et al.[13] Here, for the first time, we use a viscoelastic model based on a Burgers creep function with a distribution of relaxation times to represent both the modulus and dissipation data in an internally consistent manner.

The growing body of experimental observations thus indicates that the transition from elastic through anelastic to

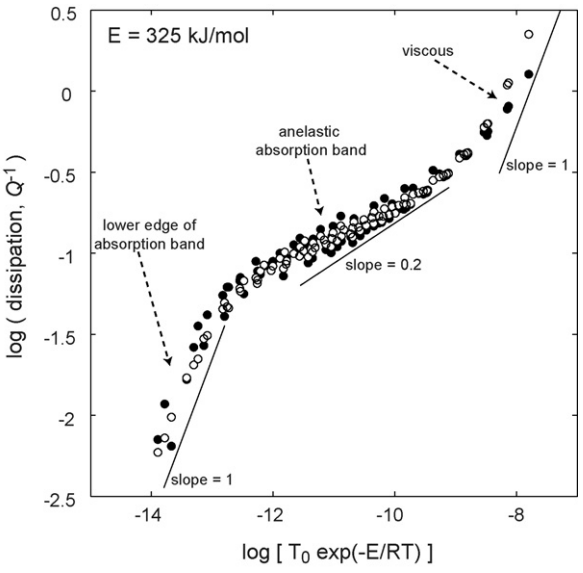

Fig. 4. Collapse of all Q^{-1} data on a master variable plot $X = T_o \exp(-E/RT)$. Solid symbols are actual data; open symbols represent the fit to the extended Burgers model (Table 2). The central part of the sigmoidal trend, of relatively shallow slope, is the broad anelastic absorption band. The steeper parts at lower and higher values of X correspond, respectively, to the lower edge of the absorption band and the onset of viscous deformation.

viscous behaviour is not satisfactorily described by the classical Raj–Ashby theory.[2]

In particular,

(i) sufficiently pure materials display no high-temperature dissipation peak attributable to elastically accommodated grain-boundary sliding;
(ii) low grain-boundary viscosity is a necessary but not sufficient condition for elastically accommodated sliding: sufficient rounding of grain edges at triple junctions is also required;
(iii) diffusional accommodation of grain-boundary sliding, presumed responsible for the high-temperature background with its mildly and monotonically frequency-dependence dissipation,[26] is ubiquitous.

These observations have provided the motivation for a new approach to the micromechanical modeling of grain-boundary sliding free from the principal limitations of Raj–Ashby theory, namely that elastic and diffusional accommodation occur separately and sequentially, and that grain edges are only moderately sharp. Preliminary results from a perturbation solution, valid only for a gently sloping periodic boundary, provide for the first time the complete relaxation spectrum.[27] As expected, the interfacial viscosity determines the behaviour at short periods T_o—with Q^{-1} increasing with increasing T_o towards the elastically accommodated sliding peak of classical theory.[2] Further increase of T_o leads to a regime beyond the peak where diffusion dominates – its influence extending progressively with increasing period from relaxation of stress concentrations at grain corners, where Q^{-1} varies only mildly with period, ultimately to grain-scale diffusion associated with steady-state creep ($Q^{-1} \sim T_o$). Significantly, the peak height varies inversely with the boundary slope, but a final answer for finite boundary slope with arbitrarily sharp grain-edge intersections awaits the results of numerical analyses in progress.

5. Conclusions

The first torsional-forced-oscillation experiments on dense, high-purity polycrystalline MgO resulted in purely elastic behaviour at temperatures $\leq$800 °C. At higher temperatures, anelastic and viscous processes contributed significant non-elastic strain. High-temperature viscoelasticity is characterised by monotonically frequency- and temperature-dependent G and Q^{-1} with no superimposed dissipation peak. In marked contrast, a previous study on lower-purity MgO[1] identified a dissipation peak now attributed to elastically accommodated grain-boundary sliding facilitated by the presence of a grain-boundary phase of low viscosity. In each case, diffusional processes are responsible for the monotonically varying dissipation background. Suppression of elastically accommodated grain-boundary sliding and the absence of a dissipation peak in pure MgO and other materials are in conflict with the classical theory for grain-boundary sliding. Alternative micromechanical models currently being developed require stringent testing against comprehensive experimental datasets, for materials like high-purity MgO with its complete range of the broad anelastic absorption band and the onset of viscous deformation, constraining not only the influence of frequency and temperature on viscoelastic behaviour, but also the effects of grain size.

Acknowledgements

Ube Materials Industries Ltd. and Prof. K. Itatani of Sophia University (Japan) are gratefully acknowledged for provision of MgO nanopowder. We thank the reviewer for the constructive review. This work was supported by Australian Research Council grant DP0450929.

References

1. Webb, S. and Jackson, I., *Phys. Chem. Min.*, 2003, **30**, 157.
2. Raj, R. and Ashby, M. F., *Met. Trans.*, 1971, **2**, 1113.
3. Raj, R., *Met. Trans. A*, 1975, **6A**, 1499.
4. Kê, T., *Phys. Rev.*, 1947, **71**, 533.
5. Mosher, D. R. and Raj, R., *Acta Metall.*, 1974, **22**, 1469.
6. Pezzotti, G., Ota, K. and Kleebe, H. J., *J. Am. Ceram. Soc.*, 1996, **79**, 2237.
7. Faul, U. H., Fitz Gerald, J. D. and Jackson, I., *J. Geophys. Res.*, 2004, **109**, B06202, doi: 10.1029/2003JB002407.
8. Pezzotti, G. K., Kleebe, H.-J., Ota, K. and Yabuta, K., *J. Am. Ceram. Soc.*, 1997, **80**, 2349.
9. Pezzotti, G. K. and Ota, K., *J. Am. Ceram. Soc.*, 1997, **80**, 2205.
10. Pezzotti, G., Kleebe, H. J. and Ota, K., *J. Am. Ceram. Soc.*, 1998, **81**, 3293.
11. Jackson, I., Faul, U. H., Fitz Gerald, J. D. and Tan, B. H., *J. Geophys. Res.*, 2004, **109**, B06201, doi:10.129/2003JB002406.
12. Lakki, A. and Schaller, R., *J. Phys.*, 1996, **IV**, 331.
13. Lakki, A., Schaller, R., Carry, C. and Benoit, W., *J. Am. Ceram. Soc.*, 1999, **82**, 2181.
14. Schlesinger, M., In *Engineered Materials Handbook*, ed. S. Schneider Jr. ASM International, 1991, pp. 883–891.

15. Itatani, K., Yasuda, R., Howell, F. S. and Kishioka, A., *J. Mater. Sci.*, 1997, **32**, 2977.
16. Bell, D., Rossman, G., Maldener, J., Endisch, D. and Rauch, F., *J. Geophys. Res.*, 2003, **108**, 2105, doi: 10.1029/2001JB000679.
17. Jackson, I. and Paterson, M. S., *Pure Appl. Geophys.*, 1993, **141**, 445.
18. Jackson, I., In Earth's deep interior: mineral physics and tomography from the atomic to the global scale, *AGU Geophysical Monograph Series 117*, ed. S. Karato, A. M. Forte, R. C. Liebermann, G. Masters, L. Stixrude, Washington DC, 2000, pp. 265–289.
19. Faul, U. H. and Jackson, I., *Earth Planet. Sci. Lett.*, 2005, **234**, 119.
20. Jackson, I., In *Advances in high-pressure technology for geophysical applications*, ed. J. Chen, Y. Wang, T. S. Duffy, G. Shen and L. F. Dobrzhinetskaya. Elsevier, 2005, pp. 95–119.
21. Anderson, O. and Isaak, D., In *Mineral Physics and Crystallography: A Handbook of Physical Constants*, ed. T. Ahrens. American Geophysical Union, Washington, 1995, pp. 64–97.
22. Zener, C., *Phys. Rev.*, 1941, **60**, 906.
23. Ghahremani, F., *Int. J. Sol. Struct.*, 1980, **16**, 825.
24. Jackson, I., Faul, U. H., Fitz Gerald, J. D. and Morris, S. J. S., *Mater. Sci. Eng. A.*, 2006, **442**, 170.
25. Cooper, R. F., In *Plastic deformation in Minerals and Rocks*, ed. S. Karato, H. Wenk, *Rev. Miner. Geochem.* 51, 2003, pp. 253–290.
26. Gribb, T. T. and Cooper, R. F., *J. Geophys. Res.*, 1998, **103**, 27267.
27. S. J. S. Morris, I. Jackson, *EOS (Trans. Am. Geophys. Union)*, 2006, **87**(52) Abstract MR21A-0009.